

OPTICAL AND X-RAY OBSERVATIONS OF IGR J00291+5934 IN QUIESCENCE

P. G. JONKER^{1,2}

SRON, Netherlands Institute for Space Research, 3584 CA Utrecht, The Netherlands; p.jonker@sron.nl

M. A. P. TORRES

Harvard-Smithsonian Center for Astrophysics, Cambridge, MA 02138; mtorres@head.cfa.harvard.edu

AND

D. STEEGHS¹

Astronomy and Astrophysics, Department of Physics, University of Warwick, Coventry CV4 7AL, UK;
 d.t.h.steeghs@warwick.ac.uk

Received 2007 November 16; accepted 2008 February 16

ABSTRACT

We report on optical and X-ray observations of the accretion-powered millisecond pulsar IGR J00291+5934 in quiescence. Time-resolved *I*-band photometry has been obtained with the 4.2 m William Herschel Telescope, while a 3 ks *Chandra* observation provided contemporaneous X-ray coverage. We found an unabsorbed 0.5–10 keV X-ray flux of $1 \times 10^{-13} \text{ erg cm}^{-2} \text{ s}^{-1}$, which implies that the source was in quiescence at the time of the optical observations. Nevertheless, the optical *I*-band light curve of IGR J00291+5934 shows evidence for strong flaring. After removal of the strongest flares, we find evidence for an orbital modulation in the phase-folded *I*-band light curve. The overall modulation can be described by effects resulting from the presence of a superhump. Comparing our light curve with that reported recently we find evidence for a change in the quiescent base level. Similar changes have now been reported for four soft X-ray transients, implying that they may be a common feature of such systems in quiescence. Furthermore, the maximum in our folded light curve occurs at a different phase than observed before.

Subject headings: accretion, accretion disks — binaries: close — stars: individual (IGR J00291+5934) — stars: neutron — X-rays: binaries

1. INTRODUCTION

Low-mass X-ray binaries (LMXBs) consist of a compact object, either a neutron star or a black hole, that accretes from a late-type companion star. The companion star typically has a mass $\lesssim 1M_{\odot}$. Stellar evolution theory predicts that neutron star LMXBs are the predecessors of the recycled millisecond radio pulsars (Radhakrishnan & Srinivasan 1982; Alpar et al. 1982). This link between the neutron star LMXBs, their transient cousins, the X-ray transients, and the millisecond radio pulsars was established by the discovery of the first accretion-powered millisecond X-ray pulsar in 1998 (Wijnands & van der Klis 1998; Chakrabarty & Morgan 1998).

Subsequently, more of these systems have been found. At the time of writing there are 10 accretion-powered millisecond X-ray pulsars known. In three of these sources pulsations are detected only intermittently (the transients HETE J1900.1–2455, Aql X-1, and SAX J1748.9–2021 in the globular cluster NGC 6440; Galloway et al. 2007; Casella et al. 2008; Altamirano et al. 2008). To date all of them are found in X-ray transients (see Wijnands 2006 for an observational overview). These transients flare up during episodes of enhanced mass accretion rate onto the neutron star. It is thought that during outburst the enhanced mass accretion rate suppresses the radio pulsar mechanism, precluding the detection of pulsed radio emission. Radio emission of these transients has been detected in outburst, but this is associated with synchrotron emission from a radio jet (e.g., SAX J1808.4–3658, Rupen et al. 2002b; XTE J0929–314, Rupen et al. 2002a; IGR J00921+5934, Pooley 2004; Fender et al. 2004). When the

mass accretion rate stops/becomes very low the radio pulsar mechanism should turn on. However, despite deep searches using sensitive radio telescopes at epochs when one of these transients, SAX J1808.4–3658, was in quiescence no radio millisecond pulsations have been found (Burgay et al. 2003). The nondetection has been ascribed to the presence of absorbing material close to the binary.

In quiescence these systems are very faint in the optical. The counterpart often cannot be detected (e.g., XTE J0929–314 and XTE J1814–331; the latter source was not detected down to $R = 23.3$; Krauss et al. 2005). For the system XTE J1751–305 the optical counterpart was not discovered in outburst nor in quiescence (Jonker et al. 2003). There are two noticeable exceptions: SAX J1808.4–3658 (Homer et al. 2001) and IGR J00291+5934 (Fox & Kulkarni 2004; Roelofs et al. 2004; Steeghs et al. 2004; Bikmaev et al. 2005). For a comprehensive overview of the outburst and initial quiescence observations of IGR J00291+5934 see Torres et al. (2008). D’Avanzo et al. (2007) recently reported multiband quiescent optical and near-infrared observations of IGR J00291+5934.

Using optical observations of SAX J1808.4–3658 in quiescence, Homer et al. (2001) found evidence for a 9%–15% semi-amplitude modulation (the observed amplitude depends on the photometric band that is used for the observations). Those authors proposed that this would be due to X-ray irradiation from the neutron star. However, as pointed out by Burderi et al. (2003), assuming that SAX J1808.4–3658 was indeed in quiescence at the time of the optical observations, the quiescent X-ray flux of SAX J1808.4–3658 is too low by 2 orders of magnitude to explain the modulation in terms of X-ray heating. The absence of a double-humped morphology rules out that the modulation is due to ellipsoidal variations. Burderi et al. (2003)

¹ Harvard-Smithsonian Center for Astrophysics, Cambridge, MA 02138.

² Astronomical Institute, Utrecht University, 3508 TA, Utrecht, The Netherlands.

proposed that the irradiation is caused by a turned-on radio pulsar instead of the quiescent X-ray emission. Evidence for a turned-on radio pulsar, albeit indirect in this case (see Campana et al. 2004), would reinforce the link between the LMXBs and the millisecond radio pulsars. Furthermore, a turned-on radio pulsar would have an important effect on the evolution of the mass-losing donor star, altering the evolutionary path of the binary (Ruderman et al. 1989). Due to the absence of pointed X-ray observations at the time of the optical observations of Homer et al. (2001) and Campana et al. (2004) low-level X-ray activity could have remained unnoticed in X-rays but would heat the side of the companion star facing the neutron star, providing an alternative explanation for the observed optical modulations. However, simultaneous X-ray and optical observations of SAX J1808.4–3658 reported by Heinke et al. (2007) forgo this possibility.

In this paper we present phase-resolved photometric observations of the optical counterpart of IGR J00291+5934 in quiescence obtained with the 4.2 m William Herschel Telescope (WHT). In addition, we present our analysis of a short contemporaneous *Chandra* observation of IGR J00291+5934 obtained with the aim to determine the contemporaneous X-ray flux.

2. OBSERVATIONS, ANALYSIS, AND RESULTS

2.1. *Chandra* X-Ray Observations

We have observed IGR J00291+5934 with the back-illuminated S3 CCD chip of the Advanced CCD Imaging Spectrometer (ACIS) detector on board the *Chandra* satellite. The observation started on 2006 September 13 at 13:33 (UTC; MJD 53,991). The data telemetry mode was set to *very faint* to allow for a thorough background subtraction. Due to windowing of the ACIS-S CCD a frame time of 0.4104 s has been used. We have reprocessed and analyzed the data using the CIAO 3.4 software developed by the *Chandra* X-ray Center using CALDB version 3.3.0.1 to take full advantage of the *very faint* data mode. In our analysis we have selected events only if their energy falls in the 0.3–7 keV range. The 0.3–7 keV background count rate was always lower than 0.4 counts s⁻¹ during our observation. The net on-source exposure time is 2.88 ks.

Using *wavdetect* we detected two sources, CXC J002911+593420 and IGR J00291+5934. We detect 22 photons from IGR J00291+5934 during the 2.88 ks observation, leading to a source count rate of 7.6×10^{-3} counts s⁻¹. Using XSPEC version 11.3.2p (Arnaud 1996) we have fitted the spectrum of IGR J00291+5934 using Cash statistics (Cash 1979) to an absorbed power-law model. We held fixed the interstellar extinction to the value of 4.6×10^{21} cm⁻² favored by Torres et al. (2008) and the power-law index to 2. We derive an absorbed 0.5–10 keV source flux of 7×10^{-14} erg cm⁻² s⁻¹ and an unabsorbed 0.5–10 keV flux of 1×10^{-13} erg cm⁻² s⁻¹. The source flux is consistent with that derived previously by Jonker et al. (2005) and Torres et al. (2008). We searched for variability in the rate of arrival of the photons, but we found none. A Kolmogorov-Smirnov (Press et al. 1992) test showed that the probability that the data are consistent with the null hypothesis of a constant photon arrival rate is 63%. We conclude that the source was in quiescence during our optical observations.

2.2. WHT Optical Observations

We obtained Harris *I*-band images using the Auxiliary Port Imager (AUX) instrument mounted on the 4.2 m WHT telescope at the Roque de Los Muchachos Observatory, La Palma, Spain. On 2006 September 13 and 14 (MJD 53,991 and 53,992 UTC) observations with an exposure time of 600 s, totaling 10.7 hr of data, were obtained. The observing conditions were good with a

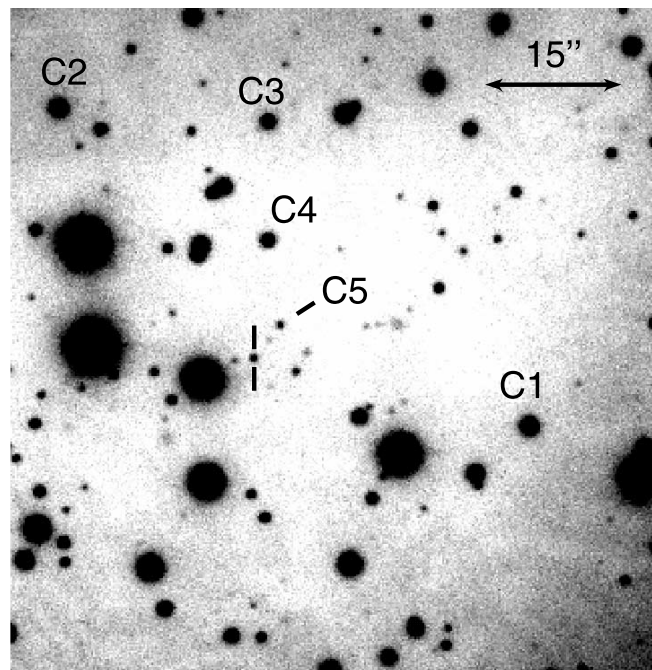


FIG. 1.—Optical *I*-band finder chart of IGR J00291+5934. North is up, and east is to the left; the scale of the image is indicated in the top-right part of the figure. The optical counterpart of IGR J00291+5934 is indicated with two vertical lines. The stars labeled C1 to C4 are comparison stars with *I*-band magnitudes 18.41 ± 0.02 , 18.55 ± 0.03 , 19.34 ± 0.05 , and 19.41 ± 0.03 , respectively. The star marked with C5 is a nearby comparison star of similar brightness as IGR J00291+5934 ($I = 21.80 \pm 0.05$).

photometric sky and a seeing varying between 0.7'' and 1.6'' and between 0.7'' and 1.0'' and with a mean seeing of 1.0'' and 0.74'' on September 13 and 14, respectively. Given the faintness of the quiescent counterpart we have rejected images with seeing $\geq 1''$. This left us with 24 images for September 13 and 40 for September 14. We used a 2×2 on-chip binning; therefore, AUX delivered a circular field of view with a diameter of 1.8' sampled at 0.22'' pixel⁻¹. Frames were debiased and then flat-fielded using dome flat-field observations.

We applied both aperture photometry and point-spread function fitting on each of the 600 s images using DAOPHOT in IRAF³ to compute the instrumental magnitudes of the detected stars. The results obtained with both methods are consistent with each other. Flux calibration of the field was performed by observing two Landolt standard stars, and differential photometry was used to derive the source flux variability as a function of time. The photometric results given here are with respect to the four field stars shown in Figure 1. These are the brightest isolated stars available in the unvignetted field of view of AUX that were recorded in the linear regime of the CCD.

We plot the *I*-band magnitude of IGR J00291+5934 (*crosses*) and those of a nearby comparison star of similar brightness (*open circles*; star C5) as observed on 2006 September 13 and 14 in Figure 2 folded on the orbital period of IGR J00291+5934. We have used the pulsar ephemeris of Galloway et al. (2005). The error in propagating the orbital ephemeris to the time of our observations is ≈ 0.01 in phase. Phase zero is superior conjunction of the neutron star (i.e., the epoch of 90° mean longitude). The brightness of the comparison star (star C5 on Fig. 1) is consistent with being constant. In contrast, the folded light curve of IGR J00291+5934 displays several large flares (see also Fig. 3). The

³ IRAF is distributed by the National Optical Astronomy Observatories.

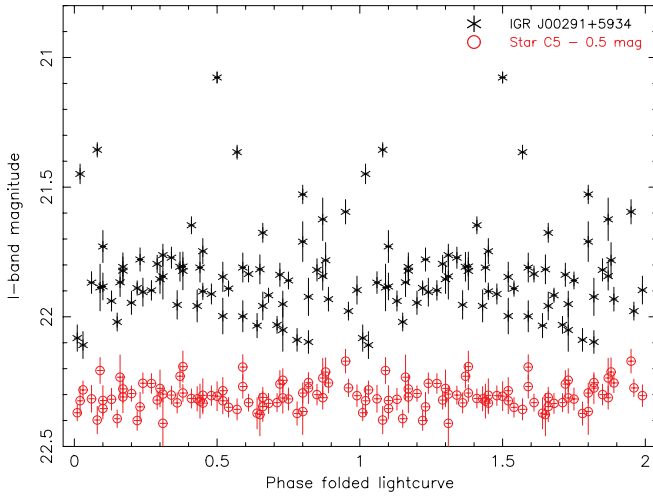


FIG. 2.—Optical *I*-band folded light curve of IGR J00291+5934 (asterisks) obtained with the 4.2 m WHT on 2006 September 13 and 14. Strong flaring of IGR J00291+5934 can be seen. The strong flaring precludes the detection of clear trends in the *I*-band magnitude as a function of orbital phase. The open circles show the *I*-band magnitude of a nearby star of comparable brightness (star C5 in Fig. 1) measured simultaneously. The points for star C5 have been scaled down by 0.5 mag for display purposes. Phase zero corresponds to the epoch of 90° mean longitude as given by Galloway et al. (2005).

average *I*-band magnitude of IGR J00291+5934 and the variance therein is 21.83 and 0.18 mag, respectively.

In an attempt to determine whether there are variations in the quiescent optical brightness due to a change in aspect of the Roche lobe-filling companion star as a function of the orbital phase, we have removed flares from the light curve of both nights. In order to come to a definition of a flare we have varied the magnitude threshold above which we identify a data point as a flare. Next, for a range of potential magnitude thresholds we fold and average the data in 10 orbital phase bins, and we determine the χ^2 and the number of degrees of freedom (dof) of a fit of a sinusoid plus a constant to the folded data. We show the results of this in Figure 4. It is clear that the χ^2 strongly decreases when more and more stringent magnitude thresholds are taken. The reduction in χ^2 levels off around a threshold magnitude of 21.75 (see Table 1). For more stringent magnitude limits the decrease in χ^2 is proportional to the reduction in the number of degrees of

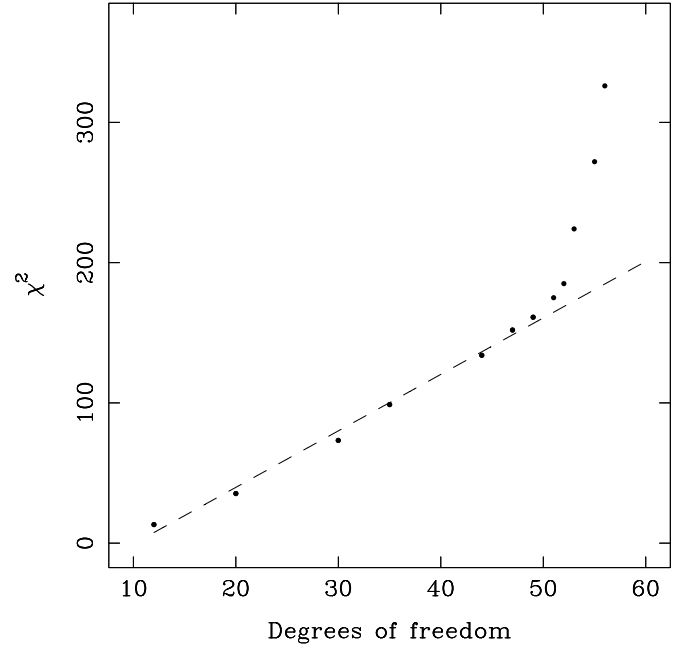


FIG. 4.—The χ^2 of the fit of a constant plus sinusoid to the phase-folded light curve of IGR J00291+5934 plotted against the number of dof in the fit for the various magnitude thresholds that we investigated (see Table 1). The drawn line is the linear correlation described by the data points below dof = 50. The transition between the linear correlation and a more steep correlation occurs around magnitude 21.75.

freedom as indicated by the straight dashed line in Figure 4. Such behavior is expected when clipping data points that are not flares.

Using 21.75 as our magnitude threshold above which we define data points as flares, the average *I*-band magnitude and the variance therein becomes 21.90 and 0.09 mag, respectively. The variance is slightly higher than ~ 0.05 , which is found for several stars of similar brightness that do not vary, implying that variability due to intrinsic variations is still present in the light curve of IGR J00291+5934. The resultant folded light curve is shown in Figure 5. The most striking feature is the presence of a clear orbital modulation. In order to quantify the modulation we have fit the folded light curve with a fit function consisting of a constant plus a sinusoid. An *F*-test gives that the improvement of a fit of a constant plus sinusoid with respect to a constant has a probability of 2% to occur due to chance. We derive $(6 \pm 1) \times 10^{-2}$ mag and 0.34 ± 0.03 for the semi-amplitude and phase of

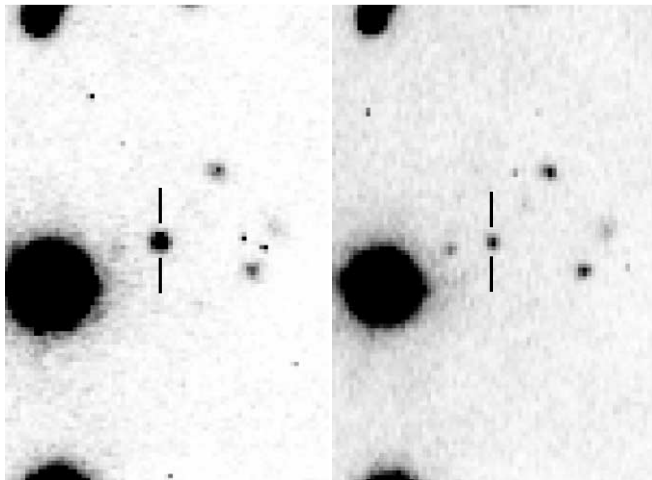


FIG. 3.—Left: Image corresponding to the strongest flare visible in Fig. 2. Right: Image taken 20 minutes after the flare. North is up, and east is to the left.

TABLE 1
THE EFFECT OF THE DEFINITION OF A FLARE ON A FIT OF A CONSTANT PLUS SINUSOID TO THE FOLDED LIGHT CURVE

Magnitude Limit	χ^2_{red}	χ^2	dof
21.95.....	1.1	13.2	12
21.90.....	1.77	35.4	20
21.85.....	2.44	73.2	30
21.825.....	2.82	98.7	35
21.80.....	3.05	134	44
21.775.....	3.23	152	47
21.75.....	3.29	161	49
21.725.....	3.43	175	51
21.70.....	3.56	185	52
21.65.....	4.23	224	53
21.60.....	4.95	272	55
21.55.....	5.82	326	56

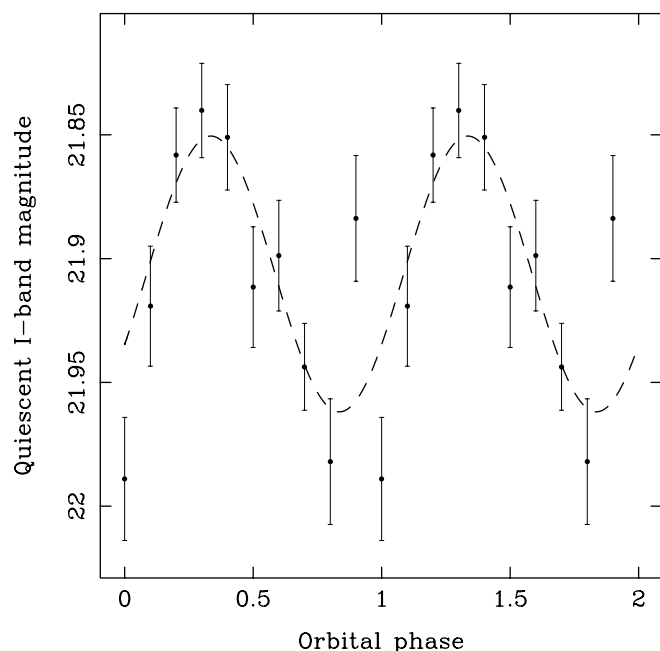


FIG. 5.—Phase-folded optical *I*-band light curve of IGR J00291+5934 after excluding flares in the light curve (i.e., data points with $I < 21.75$). The dashed line is the best-fitting model of a sinusoid plus a constant. The sinusoid reaches a maximum at phase 0.34 ± 0.03 . For clarity two orbital cycles are plotted.

the sinusoid, respectively. The value of the constant is 21.91 ± 0.01 mag. In addition to the sinusoidal variation, there is suggestive evidence for an increase in source brightness at phase 0.9. In principle, an alignment of small flares in the phase bin centered on phase 0.9 can have caused an increase above the sinusoidal modulation. Ellipsoidal modulations due to the Roche lobe-filling companion star are not detected.

3. DISCUSSION

Comparing the source X-ray flux during a 3 ks long *Chandra* observation of IGR J00291+5934 with that observed on previous occasions when the source was in quiescence, we conclude that IGR J00291+5934 was in quiescence on 2006 September 13. Optical *I*-band observations acquired with the 4.2 m WHT telescope on 2006 September 13 and 14 reveal strong variability with flares of ~ 1 mag on timescales of tens of minutes. After removal of flares we have phase folded our data. A clear sinusoidal variation is present. In our data set the orbital phase at which the source brightness is maximal is 0.34 ± 0.03 . D’Avanzo et al. (2007) report a maximum consistent with phase 0.5. Furthermore, their average *I*-band magnitude of 22.4 ± 0.2 for IGR J00291+5934 is 0.50 ± 0.22 lower than our average magnitude (after removal of flares larger than $I = 21.75$). Hence, the brightening is only significant at the 2.3σ level, and D’Avanzo et al. (2007) obtained the *I*-band observations under nonphotometric conditions. Interestingly, D’Avanzo et al. (2007) do not report evidence for flaring. The lack of flaring, together with the lower average brightness, suggests that the source showed activity at the time of our optical observations above that found by D’Avanzo et al. (2007).

In order to investigate the nature of the flares and the observed variability in the phase-folded optical light curve, we compared the quiescent properties of IGR J00291+5934 observed by us with those reported by Torres et al. (2008) and D’Avanzo et al. (2007) and with those reported for several other sources, most notably Cen X-4 (Chevalier et al. 1989; Shahbaz et al. 1993). Optical flares similar to those observed in IGR J00291+5934 in qui-

escence have been reported for several sources (e.g., Chevalier et al. 1989; Zurita et al. 2003; Hynes et al. 2003). However, flares as large as the largest that we observe in IGR J00291+5934 have not been reported to our knowledge. In addition, we note that a variation of about 0.5 mag in the average brightness similar to that mentioned above for IGR J00291+5934 has been reported for Cen X-4, XTE J2123–058 and the black hole X-ray transient A0620-00 (Chevalier et al. 1989; Tomsick et al. 2004; Cantrell et al. 2008, respectively).

Strong flares of similar duration (tens of minutes) have been observed in mid- and late-M dwarfs (e.g., see Rockenfeller et al. 2006, and references therein). However, Hynes et al. (2003) showed that the flares in quiescent LMXBs are associated with the accretion disk. Indeed, the combination of strong flaring and the lack of clear ellipsoidal variations in the phase-folded light curve (this work; D’Avanzo et al. 2007) imply that the quiescent light is not dominated by a Roche lobe-filling, but otherwise unperturbed donor star. If the flares are from the donor star, their amplitude must be larger still. Instead, (superhumps from) a residual accretion disk, the accretion stream, and/or effects from an irradiated donor star are potentially important contributors to the quiescent *I*-band light. Torres et al. (2008) derive a similar conclusion on the basis of the quiescent intrinsic $R - K$ color and constraints on the donor star from the pulsar mass function.

The absence of ellipsoidal variations in the phase-folded light curves of both IGR J00291+5934 as well as SAX J1808.4–3658 is consistent with the very low contribution of a (nonirradiated) brown dwarf to the optical light. Overall, the phase-folded quiescent *I*-band light curve of IGR J00291+5934 that we find resembles that of the average quiescent *V*-band light curve of Cen X-4 observed by Chevalier et al. (1989) in 1984–1988 (see their Fig. 7). Chevalier et al. (1989) show that a model where a large fraction of the optical light comes from the heated hemisphere of the companion star or an accretion disk attenuated by electron scattering in an accretion wake can describe the data well. In particular, such a model can explain the lower brightness at orbital phases 0.5–0.7. The heating of the companion star in millisecond X-ray pulsars in quiescence has been ascribed to the turn-on of an active radio pulsar (Burderi et al. 2003). Such an effect might be underlying the folded light curve of IGR J00291+5934; however, due to the (likely) higher level of activity during our observations additional effects seem to be important. An important clue comes from the phase difference between the maximum of the sinusoidal modulation reported by D’Avanzo et al. (2007) and that reported in this work. This suggests the presence of a modulation that has a period unequal to the orbital period, such as a superhump. Potentially, the overall morphology of our folded light curve can indeed be described by effects originating in a superhump. Superhumps have been detected in the black hole candidate XTE J1118+480 while near quiescence (Zurita et al. 2002). As explained in Whitehurst & King (1991), superhumps can occur in systems when the ratio between the companion star and the compact object mass is ≤ 0.3 . An accretion stream that perturbs the outer disk facilitates the excitation of tidal torques that are setting off the superhump resonance (Whitehurst & King 1991). The hint for a brightening of the source around phase 0.9 visible in Figure 5 can be explained by the presence of an accretion stream and hot spot, while the mass ratio is very likely (much) lower than 0.3. However, from studies of cataclysmic variables it is known that the superhump only develops during outburst, most likely since the mass and hence angular momentum transfer rate through the disk in quiescence is too low to allow for a large extent of the disk. Hence, it is not clear whether all the conditions necessary for the occurrence of superhumps are fulfilled in IGR J00291+5934 during our observations. Interestingly, Neilsen et al. (2008) also

found evidence for the presence of an eccentric, precessing disk in the black hole candidate A0620-000 in quiescence. As superhumps can potentially explain the overall variability observed in the optical in several systems while in quiescence, further investigation is necessary to test whether during phases of (enhanced) mass transfer in quiescence a superhump can develop in quiescent LMXBs with mass ratios less than 0.3.

P. G. J. acknowledges support from NASA grant G06-7032X and from the Netherlands Organisation for Scientific Research. D. S. acknowledges an STFC Advanced Fellowship. We would like to thank the referee for his/her comments that helped improve the paper.

Facilities: William Herschel Telescope, CXO (ACIS).

REFERENCES

- Alpar, M. A., Cheng, A. F., Ruderman, M. A., & Shaham, J. 1982, *Nature*, 300, 728
- Altamirano, D., Casella, P., Patruno, A., Wijnands, R., & van der Klis, M. 2008, *ApJ*, 674, L45
- Arnaud, K. A. 1996, in ASP Conf. Ser. 101, *Astronomical Data Analysis Software and Systems V*, ed. G. H. Jacoby & J. Barnes (San Francisco: ASP), 17
- Bikmaev, I., et al. 2005, *ATel*, 395, 1
- Burderi, L., Di Salvo, T., D'Antona, F., Robba, N. R., & Testa, V. 2003, *A&A*, 404, L43
- Burgay, M., Burderi, L., Possenti, A., D'Amico, N., Manchester, R. N., Lyne, A. G., Camilo, F., & Campana, S. 2003, *ApJ*, 589, 902
- Campana, S., et al. 2004, *ApJ*, 614, L49
- Cantrell, A. G., Bailyn, C. D., McClintock, J. E., & Orosz, J. A. 2008, *ApJ*, 673, L159
- Casella, P., Altamirano, D., Patruno, A., Wijnands, R., & van der Klis, M. 2008, *ApJ*, 674, L41
- Cash, W. 1979, *ApJ*, 228, 939
- Chakrabarty, D., & Morgan, E. H. 1998, *Nature*, 394, 346
- Chevalier, C., Ilovaisky, S. A., van Paradijs, J., Pedersen, H., & van der Klis, M. 1989, *A&A*, 210, 114
- D'Avanzo, P., Campana, S., Covino, S., Israel, G. L., Stella, L., & Andreuzzi, G. 2007, *A&A*, 472, 881
- Fender, R., De Bruyn, G., Pooley, G., & Stappers, B. 2004, *ATel*, 361, 1
- Fox, D. B., & Kulkarni, S. R. 2004, *ATel*, 354, 1
- Galloway, D. K., Markwardt, C. B., Morgan, E. H., Chakrabarty, D., & Strohmayer, T. E. 2005, *ApJ*, 622, L45
- Galloway, D. K., Morgan, E. H., Krauss, M. I., Kaaret, P., & Chakrabarty, D. 2007, *ApJ*, 654, L73
- Heinke, C. O., Deloye, C. J., Jonker, P. G., Taam, R. E., & Wijnands, R. 2007, in AIP Conf. Proc. 983, *40 Years of Pulsars: Millisecond Pulsars, Magnetars, and More*, ed. C. Bassa et al. (New York: AIP), 526
- Homer, L., Charles, P. A., Chakrabarty, D., & van Zyl, L. 2001, *MNRAS*, 325, 1471
- Hynes, R. I., Charles, P. A., Casares, J., Haswell, C. A., Zurita, C., & Shahbaz, T. 2003, *MNRAS*, 340, 447
- Jonker, P. G., Campana, S., Steeghs, D., Torres, M. A. P., Galloway, D. K., Markwardt, C. B., Chakrabarty, D., & Swank, J. 2005, *MNRAS*, 361, 511
- Jonker, P. G., et al. 2003, *MNRAS*, 344, 201
- Krauss, M. I., et al. 2005, *ApJ*, 627, 910
- Neilsen, J., Steeghs, D., & Vrtilak, S. D. 2008, *MNRAS*, 384, 849
- Pooley, G. 2004, *ATel*, 355, 1
- Press, W. H., Teukolsky, S. A., Vetterling, W. T., & Flannery, B. P. 1992, *Numerical Recipes in FORTRAN: The Art of Scientific Computing* (2nd ed.; Cambridge: Cambridge Univ. Press)
- Radhakrishnan, V., & Srinivasan, G. 1982, *Curr. Sci.*, 51, 1096
- Rockefeller, B., Bailer-Jones, C. A. L., Mundt, R., & Ibrahimov, M. A. 2006, *MNRAS*, 367, 407
- Roelofs, G., Jonker, P. G., Steeghs, D., Torres, M., & Nelemans, G. 2004, *ATel*, 356, 1
- Ruderman, M., Shaham, J., Tavani, M., & Eichler, D. 1989, *ApJ*, 343, 292
- Rupen, M. P., Dhawan, V., & Mioduszewski, A. J. 2002a, *IAU Circ.* 7893, 2
- Rupen, M. P., Dhawan, V., Mioduszewski, A. J., Stappers, B. W., & Gaensler, B. M. 2002b, *IAU Circ.* 7997, 2
- Shahbaz, T., Naylor, T., & Charles, P. A. 1993, *MNRAS*, 265, 655
- Steeghs, D., Blake, C., Bloom, J. S., Torres, M. A. P., Jonker, P. G., & Starr, D. 2004, *ATel*, 363, 1
- Tomsick, J. A., Gelino, D. M., Halpern, J. P., & Kaaret, P. 2004, *ApJ*, 610, 933
- Torres, M. A. P., et al. 2008, *ApJ*, 672, 1079
- Whitehurst, R., & King, A. 1991, *MNRAS*, 249, 25
- Wijnands, R. 2006, in *Trends in Pulsar Research*, ed. J. A. Lowry (New York: Nova Sci.), 53
- Wijnands, R., & van der Klis, M. 1998, *Nature*, 394, 344
- Zurita, C., Casares, J., & Shahbaz, T. 2003, *ApJ*, 582, 369
- Zurita, C., et al. 2002, *MNRAS*, 333, 791